JOC The Journal of Organic Chemistry

Article

Visible-light photocatalytic synthesis of amines from imines via transfer hydrogenation using quantum dots as catalysts

Zi-Wei Xi, Lei Yang, Dan-Yan Wang, Chaodan Pu, Yong-Miao Shen, Chuan-De Wu, and Xiaogang Peng

J. Org. Chem., **Just Accepted Manuscript** • DOI: 10.1021/acs.joc.8b01651 • Publication Date (Web): 31 Aug 2018

ACS Publications

is published by the American Chemical Society. 1155 Sixteenth Street N.W., Washington, DC 20036

Visible-light photocatalytic synthesis of amines from imines via transfer hydrogenation using quantum dots as catalysts

Zi-Wei Xi[†,‡], Lei Yang[†,†], Dan-Yan Wang[ǁ], Chao-Dan Pu[*,†], Yong-Miao Shen[*,†,‡,ǁ], Chuan-De Wu[†], Xiao-Gang Peng[†]

[†]Center for Chemistry of Novel & High-Performance Materials, Department of Chemistry, Zhejiang University, Hangzhou, 310027, P. R. China

[‡]Department of Chemistry and Chemical Engineering, Shaoxing University, Shaoxing, 312000, P. R. China

[ǁ]Department of Chemistry, Zhejiang Sci-Tech University, Hangzhou, Zhejiang 310018, P. R. China

Table of Contents Graphic:

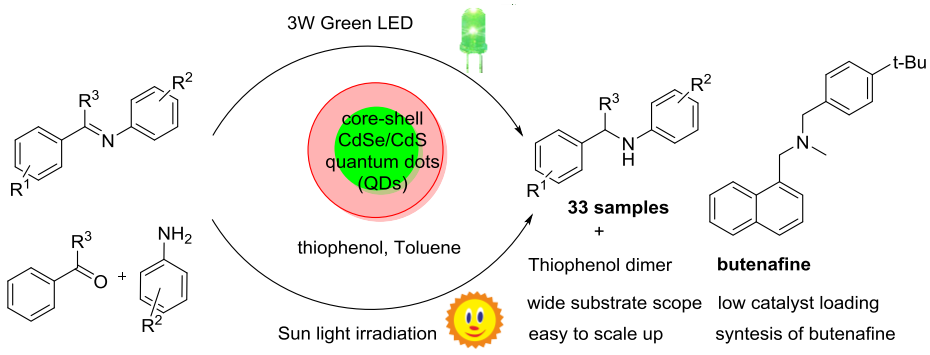

ABSTRACT: CdSe/CdS core/shell quantum dots (QDs) can be used as stable and highly active photoredox catalysts for efficient transfer hydrogenation of imines to amines with thiophenol as a hydrogen atom donor. This reaction proceeds via a proton coupled electron transfer (PCET) from the QDs conduction band to the protonated imine followed by hydrogen atom transfer from the thiophenol to the α-aminoalkyl radical. This precious metal free transformation is easy to scale up and can be carried out by a one-pot protocol directly from aldehyde, amine and thiophenol. Besides, other advantageous features of this protocol include a wide substrate scope, high yield of the amine products, extremely low catalyst loading (0.001 mol %), high turnover number (10^5) and the mild reaction conditions of using visible light or sun light at room temperature in neutral media.

Introduction

Aliphatic amines are ubiquitous building blocks in organic synthesis and exist as core structures in a variety of natural products, pharmaceuticals, and agrichemicals. [1] The overwhelming importance of amines demands development of effective and diversity-oriented synthetic methods. Among present approaches, hydrogenation and transfer hydrogenation of imines constitute one of the most efficient and straightforward synthetic routes, which can be realized by transition metal catalysis, [2] organocatalysis, [3] and metal-organo cooperative catalysis. [4] However, these reactions suffer from several shortcomings and limitations that often hamper their practical applications, such as the high cost of the precious metal catalysts, relatively low catalyst activity and turnover number caused by coordination or reaction of the amine products with the catalysts, limited diversity of organocatalysts, harsh reaction conditions and narrow substrate scope. It is therefore desirable to develop new, efficient, and versatile imine reductive hydrogenation methods not relying on precious metal complexes as catalysts.

By application of a series of visible-light responsive photocatalysts, including ruthenium and iridium coordination compounds, [5] as well as organic dyes, [5b,6] visible-light photoredox catalysis has recently been actively investigated and established as a powerful technique to induce a myriad of radical based reactions. In this regard, imine has been reported to take part in photoredox catalyzed alkylation, [7] allylation, [8] aminoalkylation, [9] arylation, [10] dimerization, [11] and inverse hydroboration. [12] Most recently, three reports on photoredox transfer hydrogenation of diarylketoimines have appeared, all using iridium complex—$[Ir(ppy)_2(dtbbpy)]^+(PF_6^-)$ or a sulfonated Ir *fac*-$Ir(ppy)_3$—as photocatalyst.[13] In addition, photocatalyzed synthesis of aliphatic amines has been reported by using iridium complex $Ir[dF(CF_3)ppy][bpy]PF_6$ and ruthenium complex $Ru(bpy)_3Cl_2$ as photocatalyst respectively through aldehyde and ketone reductive amination reactions.[14]

Colloidal semiconductor nanocrystals with their sizes in quantum-confinement regime (quantum dots, QDs) have recently emerged as a class of potential photocatalysts owing to their excellent electronic and structure properties, i.e. wide and strong absorption for light harvesting, size dependent band gap for tunable and selective driving force of redox reaction, large surface-to-volume ratio for charge extraction and rich reaction sites, and potentially good photochemical stability. [15] Studies in this area have so far focused on hydrogen production via water splitting, and the photodegradation of organic molecules. [16] Recently, a few reports have studied application of QDs in photocatalytic organic reactions of synthetic interest, such as reduction of aromatic nitro compounds and azides to amines, [17] debromination and C−H arylation reactions of aryl bromides,[18] and other C−C bond forming reactions.[19] Kisch and Shiraishi had reported that semiconductors can catalyze imine reductive reactions. But most of these reactions were performed under UV irradiation with high catalyst loadings.[20] It should be noted that, in most of these studies, plain core QDs have been applied as photocatalysts be-

cause extraction of photo-generated carriers from core/shell QDs with type-I band offsets is believed to be difficult. [21] However, photo-stability and chemical-stability (such as aggregation and etching) of plain QDs have frequently been problematic during photocatalytic reactions, while better stability and control of carrier dynamics of core/shell QDs render them advantages as catalysts for photocatalytic reaction. [22]

In this work, nearly defect-free CdSe/CdS core/shell QDs were explored as photocatalysts for transfer hydrogenation reaction of imines with thiophenol as hydrogen source for a wide scope of amines. In comparison with the plain core CdSe QDs, CdSe/CdS core/shell QDs were stable yet efficient as photocatalysts in the series of reactions studied. Comparing to the iridium complex catalyzed hydrogenation of imines, our protocol is a precious-metal free reaction with a wider substrate scope, applicable not only to diaryl and aryl-alkyl ketoimines, but also to a diversity of aldimines.

Results and Discussion

All QDs used in this work were prepared according to our previously published method. [23] The size of plain CdSe and CdSe core in core/shell QDs was about 3 nm in diameter, with first absorption at 550 nm. CdS was chosen as shell materials because of the superior optical properties and well established synthetic methods of CdSe/CdS core/shell QDs. We started our optimization studies by reduction of 4-fluoro-*N*-(4-fluorobenzylidene)aniline **1k** in the presence of **2a** in toluene. Reaction conditions were screened by use of various hydrogen donors in varying amounts. We found that for CdSe/CdS core/shell QDs with 3 monolayers of CdS shell, 7 eq. of 4-fluorothiophenol with 8 h visible light irradiation could give satisfactory result (Table 1, entry 8). The catalyst could be applied at extremely low loading (0.001 mol %) to lead to effective reactions, indicating a turnover number of about 10^5. It should be noted that this is not the maximum turnover number since our QDs were still stable after reaction (see below).

When CdSe/CdS core/shell QDs with 5 monolayers of CdS shells were chosen as the photocatalyst, the yield decreased slightly (Table 1, entry 10). The yield decreased noticeably when we used the same amount of plain core CdSe QDs as the catalyst (Table 1, entry 11). We also checked reactions catalyzed by CdS QDs under the standard reaction conditions, which gave about 60% yield. Moreover, plain CdSe core precipitated during the reaction. Overall, both photocatalytic efficiency and stability of core/shell QDs were much better than those of the plain core QDs, indicating that charge extraction was not the determinant factor for practical photocatalytic use of these QDs as the catalysts. When we using mercaptan as a hole scavenger, the yield was decreased significantly (Table 1, entry 15, 16, 17). The reaction could not proceed by using triethanolamine or triethylamine as a hole scavenger, because of its low ability to extract hole from QDs (Table 1, entry 18, 19). Control experiments confirmed that

presence of QDs and thiophenol was essential for the reactions to occur (Table 1, entry 13). Also, the reaction could not proceed in the dark (Table 1, entry 14).

Table 1. Selected Optimization Experiments[a]

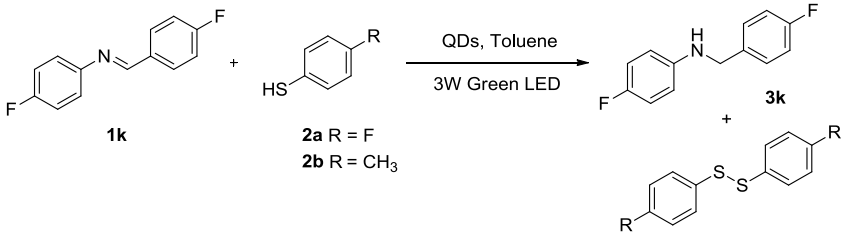

entry	catalyst ($\times10^{-3}$ mol %)	hole acceptor (equiv)	reaction time (h)	yield (%)
1	2	**2a** (5)	10	63
2	2	**2a**(7)	10	69
3	2	**2a** (9)	10	65
4	2	**2a** (7)	6	58
5	1	**2a** (7)	10	84
6	1	**2b** (7)	10	37
7	0.5	**2a** (7)	8	82
8	1	**2a** (7)	8	87
9	1.5	**2a** (7)	8	82
10	1[b]	**2a** (7)	8	78
11	1[c]	**2a** (7)	8	60
12	1[d]	**2a** (7)	8	60
13	1	0	8	0
14	0	**2a**(7)	8	0
15	1	(4-chlorophenyl)methanethiol (7)	8	10.7[e]
16	1	1-hexylthiol	8	3.8[e]
17	1	1,3-dimercaptopropane	8	20.7[e]
18	1	Triethanolamine (7)	8	0
19	1	Triethylamine (7)	8	0

[a]Reactions performed with imine **1k** (0.4 mmol, 86.8 mg), QDs with 3 monolayers of CdS (2×10^{-5} mol/L), **2**, toluene 8 mL, purging with Argon gas for 10 minutes before illumination with 3 W Green LED. [b]The QDs with 5 monolayers of CdS as the photocatalyst. [c]CdSe Core as the photocatalyst. [d] CdS QDs as the photocatalyst. [e] Determined by GC-MS.

With the optimal reaction conditions established, we first explored the reaction scope for aldimines (Table 2). We found that for all aldimines tested, full conversion could be reached by 6 to 10 hours irradiation. The substituent effects on both the *N*-aryl and *C*-aryl were examined. Most of the reactions proceeded with more than 80% yield whether the substituent was electron-rich (entry 1, 2, 6, 7, 16, 25)

or electron-deficient (entry 4, 4, 11-15, 20, 24) on either of the phenyl rings. The position and the number of the substituents on the phenyl rings showed no significant effect on yield (entry 13, 14). The stability of the imine in the reaction solution was the most important factor affecting the reduction yield. For example, 4-acetyl substituent on the aniline moiety gave 79% yield of the amine with a 6% decomposition of the starting imine according to GC-MS measurements. The relatively low yield (40%) for **3t** was also a result of the gradual decomposition of the imine during the reaction course. We then extended the reaction to the *N*,*N'*-dibenzylidene-1,4-phenylenediamine and this diamine was smoothly reduced to the diamine **4** in 72 % yield (Scheme 1).

Table 2. Scope of Aldimines[a]

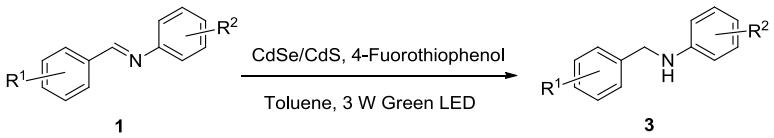

entry	**1**	R^1	R^2	**3**	Yield/%
1	**1a**	H	H	**3a**	88
2	**1b**	H	4-OH	**3b**	83
3	**1c**	H	4-OMe	**3c**	84
4	**1d**	H	4-F	**3d**	82
5	**1e**	H	4-Cl	**3e**	90
6	**1f**	4-Me	4-OMe	**3f**	93
7	**1g**	4-Me	4-Me	**3g**	88
8	**1h**	4-Me	4-F	**3h**	82
9	**1i**	4-Me	4-Cl	**3i**	86
10	**1j**	4-F	4-OMe	**3j**	94
11	**1k**	4-F	4-F	**3k**	86
12	**1l**	4-F	4-Cl	**3l**	92
13	**1m**	4-Cl	4-F	**3m**	81
14	**1n**	2-Cl	4-F	**3n**	88
15	**1o**	4-Cl	4-Cl	**3o**	82
16	**1p**	4-OMe	4-Me	**3p**	86
17	**1q**	4-OMe	4-F	**3q**	93
18	**1r**	4-OMe	4-Cl	**3r**	82
19	**1s**	4-OMe	4-COMe	**3s**	68
20	**1t**	4-CN	4-CN	**3t**	40
21	**1u**	4-$PhCH_2O$	4-F	**3u**	85
22	**1v**	4-F	3,4-diMe	**3v**	90
23	**1w**	4-(n-$C_6H_{13}O$)-	4-CN	**3w**	85

24	**1x**	4-CF_3	4-F	**3x**	82
25	**1y**	4-OMe	4-OMe	**3y**	87

[a]Reactions performed with imine **1** (0.4 mmol, 86.8 mg), QDs with 3 monolayers of CdS (4×10^{-9} mol, 2×10^{-5} mol/L, 1×10^{-3} mol %) and 4-fluorophenyl thiophenol (2.8 mmol, 0.359 g, 7 eqiv) in toluene (8 mL), purging with argon gas for 10 minutes before illumination by 3 W green LED.

We further found that, not only *N*-aryl aldimines, but also *N*-alkyl aldimines were suitable substrates (Scheme 1), affording the corresponding amine products in moderate to high yield (**5** and **6**). We then tested the reactions of several diaryl and aryl alkyl ketimines and it turned out that these ketimines behaved equally well and were reduced in good yields (**7**, **8**, **9**).

Scheme 1. Scope of Imines

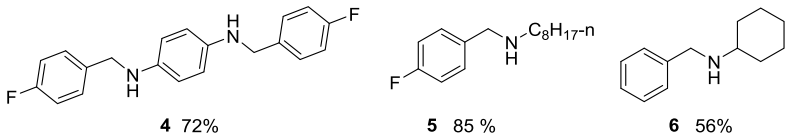

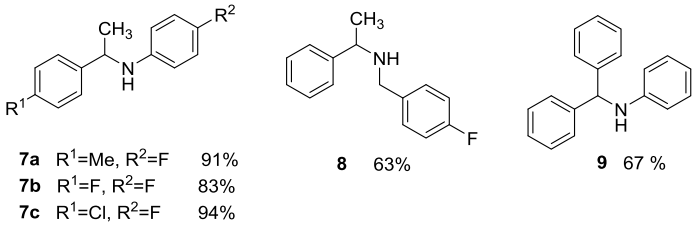

The reaction is easy to scale up. When we carried out a gram scale reduction of benzylidene-4-fuoroaniline under the standard reaction conditions using a 20 W green LED as light source, the product **3d** was isolated in 83 % yield (Scheme 2a). Moreover, direct one-pot reaction between an benzaldehyde, an aniline and 4-fuorothiophenol proceeded smoothly to give excellent yields of products **3a** (76 %), **3d** (87 %), **3g** (93%) although the reaction took 16 h to be completed, twice that using the imine directly (Scheme 2b). The one-pot reactions can also proceed with aliphatic amines as the starting material, and also give satisfactory yields (products **5** and **6**).

As an example to show the potentiality of this reaction for the synthesis of biologically active amines, we successfully accomplished the synthesis of the antimycotic agent butenafine by using a direct one-pot reaction between 1-naphthalene aldehyde, 4-*t*-butylbenzylamine and 4-fuorothiophenol. This gave the reduction product in 86% yield. Subsequent direct methylation under non-optimized conditions gave the butenafine **10**. The overall yield of **10** covering the photoreduction and methylation is 65%.

Scheme 2. Practical Applications of the Reaction a) a gram scale reaction. b) one-pot reaction. c) butenafine synthesis.

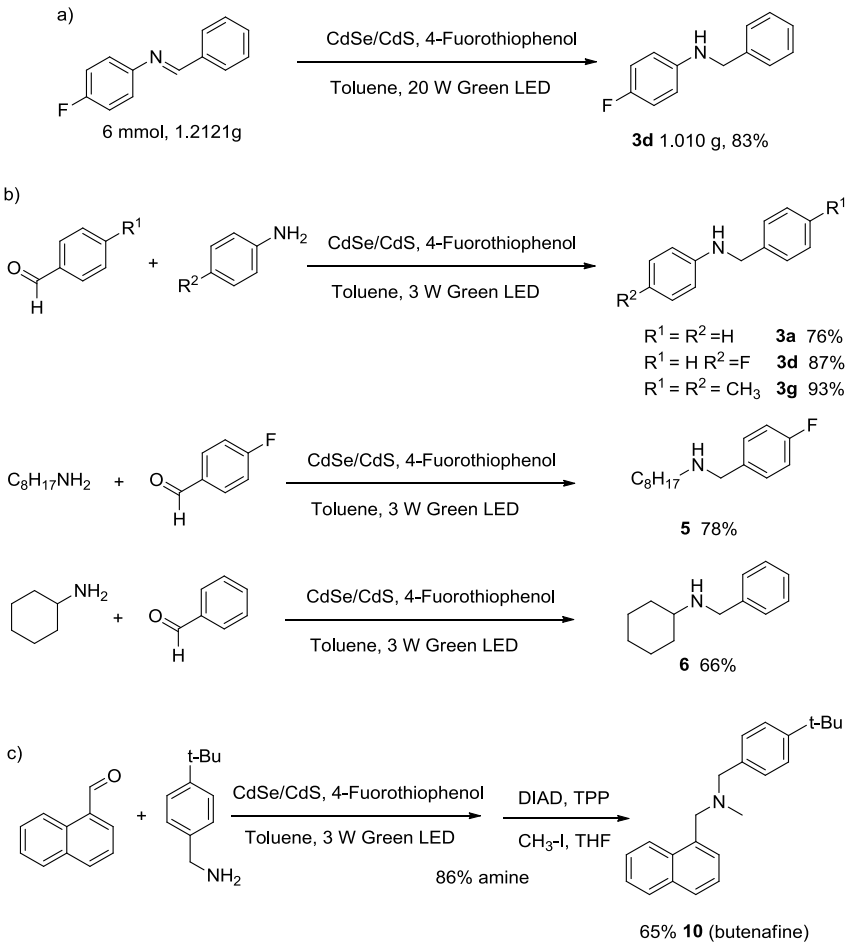

Use of sun light as a light source was tested. It was found that the reaction proceeded swiftly under solar irradiation and it took only 3 hours in a clear day to reach a completion to give the product **3d** in 84% yield (For additional experimental details, see Supplementary Information).

The QDs are very stable in the reaction system, i.e., remaining colloidal stability and no detectable decrease in activity even after 24 hours illumination (Figure 3s). TEM images show that the shape and size of the QDs showed no obvious change after reactions (Figure 1). Compared to imine, the amount of the QD used is only 0.001 mol %. It is therefore quite hard to collect and to recycle the catalyst. However, QDs still have the ability to photocatalyze the reaction when the starting materials were added to the solution again.

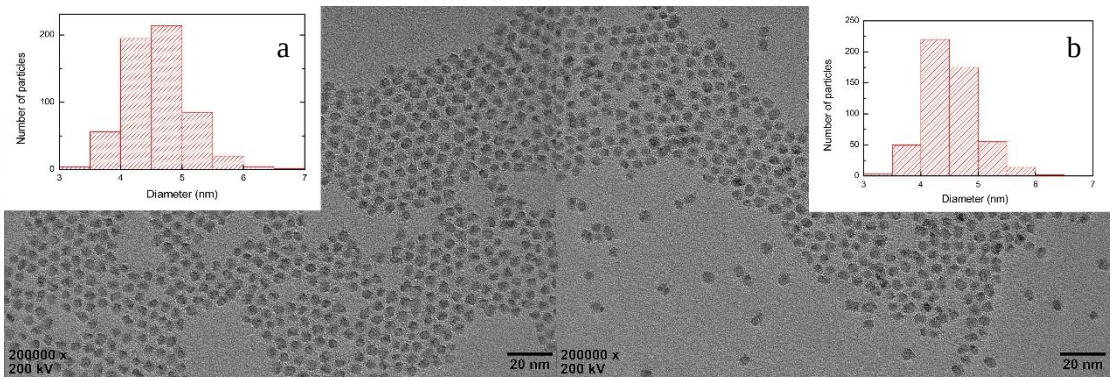

Figure 1. TEM images of CdSe/3CdS before (a) and after (b) the reaction.

Several experiments were carried out to clarify the reaction mechanism. Deuterium labeling experiments were carried out to confirm the hydrogen source. When the reaction was conducted under standard conditions with deuterated thiophenol, almost no deuterium was detected in final products. In this case, it is obvious that deuterium exchange between the deuterated thiophenol and the ligands in QD catalyst results in a diminished deuterium incorporation into the imine reduction products. However, when QDs were pre-deuterium labeled with deuterated isopropanol, almost 70% deuterium incorporation was observed at the methylene and amino position (Scheme 3b). It should be noted that the amount of deuterium in the prepared deuterated thiophenol was also about 70%. No deuterium incorporation was observed with toluene-d_8 as the reaction solvent (see Figure 7s, 8s in supporting information). All these results demonstrated that thiphenol was the hydrogen source.

Scheme 3. Deuterium Incorporation Studies

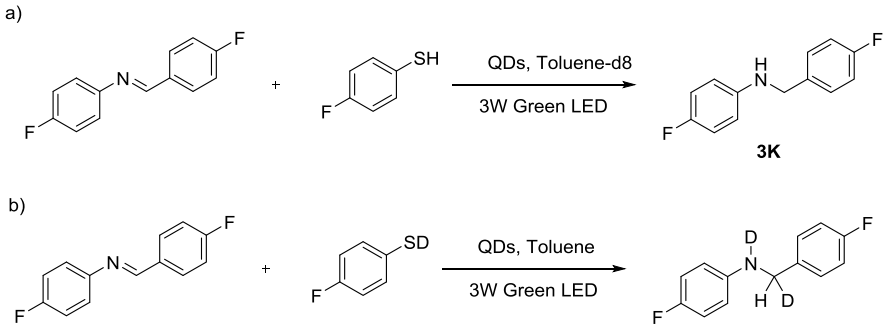

When a stoichiometric amount of radical scavenger 2,2,6,6-tetramethylpiperidine *N*-oxide (TEMPO) was added to the reaction, no desired product was detected. The TEMPO-thiophenol adduct was formed in 28% yield judged from the amount of TEMPO (Scheme 4, determined by GC-MS). Meanwhile, the imine remained unchanged during the reaction.

Scheme 4. Trapping of the Radical

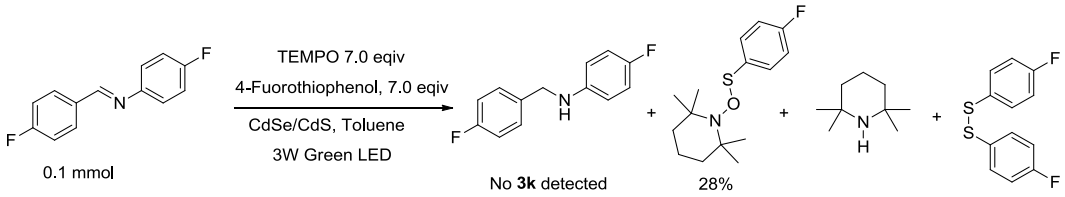

Fluorescence quenching experiments were conducted with the imine **1k** and thiophenol **2a** as the QDs quencher, respectively (Figure 2). Thiophenol behaved as strong quencher of QDs (5.68×10^{9} L/mol•s) while the imine quenched the fluorescence weakly (1.95×10^{8} L/mol•s). However, thiolate should be a stronger quencher than thiophenol. The ligand of our core/shell QDs were mostly oleylamine. Considering the relatively strong acidity of the thiophenol (pK_a 10.3 in DMSO, as comparing with the18.0 and 15.4 for the less acidic phenol and aliphatic thiol, respectively)[24] proton transfer may take place between the oleyl amine ligand in QD and the absorbed thiophenol. Indeed, we found that, thiolate anions were formed when thiophenol was mixed with oleylamine in solution (See Figure 9s in the Supplementary Information). We therefore believe that thiolate plays an important, if not dominant role as hole trap in the quenching process. This conclusion is also supported by the well correlated conversion yields with the acidity of the thiophenols shown in Table 1 where using the more acidic 4-fluorothiophenol gave a much higher yield of product (84%) than using the less acidic 4-methylthiophenol (37%), while the aliphatic thiols which are least acidic and have higher oxidation potential (1.12 V, SCE)[25] fail to afford any product.

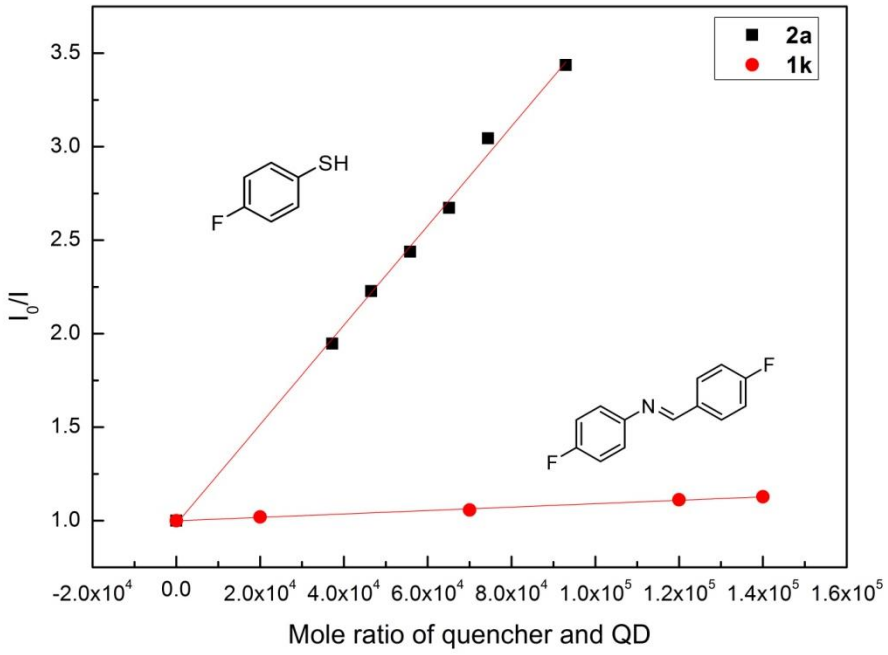

Figure 2 Fluorescence quenching data of 4-fluorothiophenol and imine(**1K**).

The role of hole trapping in the reaction may also be the reason for the insensitivity of this photocatalytic system to imine substrates and the better photocatalysis efficiency for CdSe/CdS core/shell QDs than plain core. The CdSe/CdS core/shell QDs has quasi-type II structure with hole localized in the CdSe core and electron delocalized in the whole QDs. As a result, when hole was efficiently extracted by thiol/thiolate, the subsequent electron transfer would be easy. Considering the moderate photocatalysis efficiency of CdS QDs, we carried out the reaction by irradiation with yellow light, we still obtain high conversion yield using core/shell QDs, while the yield of using CdS QD was almost zero. This means that the higher catalytic efficiency is a result of core/shell structure. CdS shell could protect photo-induced charge from being trapped by surface defects, which would improve the photocatalysis efficiency of core/shell QDs and eliminate undesirable surface reactions, such as degradation of surface ligands.

Based on these results, a plausible mechanism for the photo catalytic transfer hydrogenation of imines to amines is suggested in Scheme 5. The first step should be absorption of visible light by CdSe/CdS core/shell QDs to generate an electron-hole pair. [26] Holes were transferred from the valence band to thiolate (route 1 in Scheme 5) and thiophenol (route 2 in Scheme 5) to generate the thiyl radical either directly or by the deprotonation of the thiophenol cation radical. This was not only supported by the fluorescence-quenching studies but also backed up by the match of the QDs reduction potential (∼0.9 V) (see the supporting information for additional details) [27] and oxidation potentials of the thiolate (-0.85 V) and thiophenol (0.95 V [25]). Meanwhile, reduction of the weak electron acceptor imine (typical reduction potential of aldimins is about -2 V [28]) by electrons in QDs' conduction band (∼-1.2V)[25] should be thermodynamically unfavorable. Proton transfers from the protonated oleylamine and thiophenol to the imine coupled with electron transfer from the conduction bond of QDs to the protonated imine gives the radical intermediate **A**. Hydrogen atom transfer (HAT) from a second thiophenol molecule affords the terminal product and another thiyl radical. The thiyl radical dimerization leads to the disulfide.

Scheme 5. Mechanistic Hypothesis for Photoredox-Transfer Hydrogenation Reaction

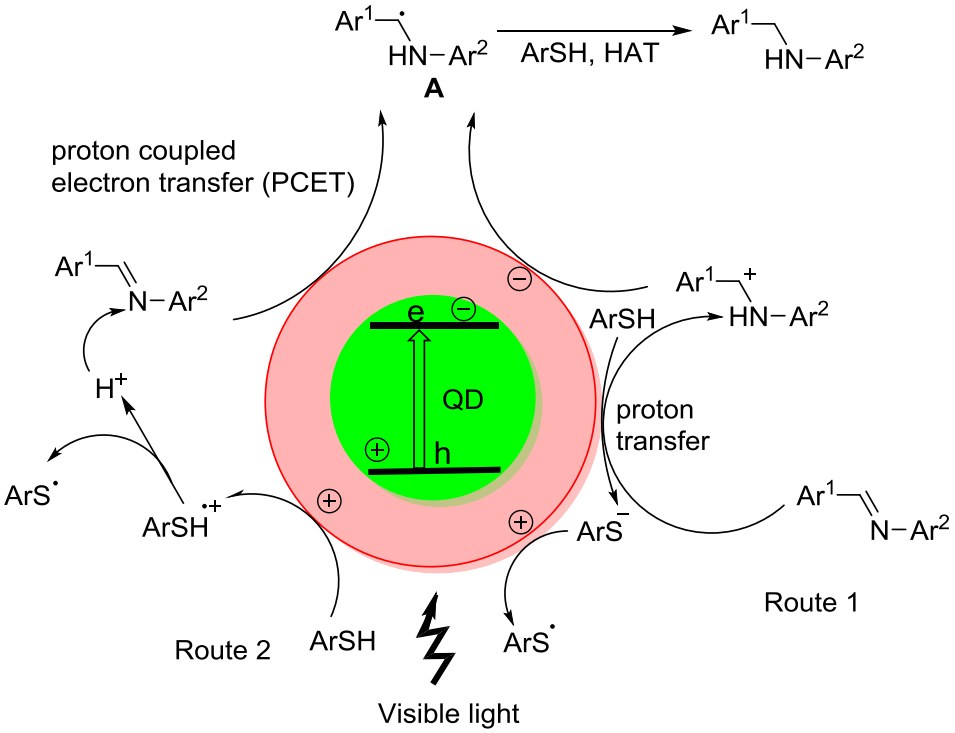

Conclusions

In summary, CdSe/CdS core/shell QDs are proven to be stable and highly active photocatalyst in place of precious metal complexes and organic dyes for visible light induced transfer hydrogenation reactions of imines to amines. We show here that the strong and much wider absorption of QDs in the whole visible light region may enable them more efficient and practical for use in catalyzing organic transformations than transition metal complex. Also, band structure and wavefunction engineering may render them more versatile photocatalytic activity. The improved stability of core/shell QDs than plain QDs also makes the former advantageous as photocatalysts for a wide range of reactions. Besides illustrating the potential of core-shell QDs as photoredox catalyst for organic transformations, practical synthetic value of this precious metal free protocol is manifested by the fact that it has a wide imine substrate scope, including both aldimine and ketimines of diversified structures to give satisfactory yield of the amines under mild reaction conditions by using visible light or sun light at room temperature in neutral media.

EXPERIMENTAL SECTION

All reagents were commercially available and used without further purification. All solvents were dried according to standard procedures, and further dried by 4 Å molecular sieves. Melting points were measured on a microscopic melting point apparatus and are uncorrected. ^{1}H and ^{13}C NMR spectra were recorded at 400 and 100 MHz, respectively, using $CDCl_3$ or DMSO-d_6 as solvent. IR spectra were taken with a FT-IR spectrometer. HRMS was determined by a AB Triple TOF 5600 plus System. The exact mass calibration was performed automatically before each analysis em-

ploying the Automated Calibration Delivery System. UV–vis absorption spectra were measured on a UV–vis spectrometer. Fluorescence spectra and time-dependent single photon count spectra were measured on a FL900 Instrument.

General procedures for photoredox transfer hydrogenation

A mixture of imine **1** (0.4 mmol, 1.0 equiv) and 4-fluorothiophenol (0.358 g, 2.8 mmol, 7.0 equiv) in toluene (8 mL) was added QDs (200 μL) as photocatalyst. The vial was sealed and the reaction mixture sparged with argon for 10 minutes and then irradiated with 3 W green LEDs. After 8 h, the mixture was concentrated by rotary evaporation and the crude mixture was directly charged on silica gel and purified by column chromatography with petroleum ether/ethyl acetate as eluents (gradient elution) to afford the target product.

General procedures for the synthesis of QDs [23a, 23b, 30, 31]

Synthesis of 3.0 nm CdSe QDs (first exciton absorption peak at 550 nm) was achieved by a modified literature procedure[1]. Cadmium acetate (0.0533 g, 0.2 mmol) and stearic acid (0.1707 g, 0.6 mmol) were loaded into a 25 mL three-neck flask with 4 mL of ODE. After stirring and argon bubbling for 10 min, the mixture was heated to 270 ℃ by a digital-controlled heating mantle to remove excess HAC and form a colorless solution. The temperature was reduced to 250 ℃, and 1 mL of the Se-Sus was injected quickly into the hot solution. The reaction temperature was kept at 250 ℃ for further growth of the QD. After growth for ~7 min, 0.05 mL of Se-Sus was injected into the reaction solution. Multiple injections were repeated every 2−3 min until the size of the QDs reached 3.3 nm. Needle-tip aliquots were taken and dissolved in toluene for UV−vis and fluorescence spectra measurements to monitor the reaction.

Synthesis of CdSe/3CdS core/shell QDs were carried out according to previously published single-precursor approach [23b, 30]. Briefly, dodecane (1.5 mL), oleylamine (3.8 mL), and purified CdSe core (containing about 6×10^{-8} mol of nanocrystals) were added to a three-neck flask under argon flow and then heated to 80 ℃. $Cd(DDTC)_2$ was used as the single precursor for CdS shell growth. For each monolayer, addition of the precursor solutions was at 80 ℃ and growth was at 160 ℃ for 20 min. The amount of the $Cd(DDTC)_2$-amine solution (0.15 M) for each injection was estimated by extinction coefficients and calibrated by the TEM measurements. For a reaction with 6×10^{-8} mol of 3.0 nm CdSe core, the amount for three consecutive injections of the precursor solution was calibrated as 0.08, 0.12, and 0.17 mL, respectively. After the targeted shell thickness was achieved, the reaction was stopped and the solution was allowed to be cooled to room temperature.

Synthesis of 5 nm CdS QDs[23e] were carried out by injecting S-ODE (0.05 mmol S in 0.5 mL ODE) to the mixture containing ODE (3 mL), cadmium oxide (0.2 mmol) and oleic acid (0.6 mol) at 230 ^{o}C. Reaction temperature was then set at 250 ^{o}C and maintained for 20 min. Then S-ODE (0.005 mmol S in 0.05 mL ODE) was injected at interval of 2.5 min until the first absorption peak reached 455 nm.

Purification of the Core/Shell QDs [23a, 31]:

In order to retain the PL properties, a recently developed purification procedure was applied n precipitation of the core/shell QDs from the reaction solution. Briefly, the crude reaction solution was mixed with acetonitrile (1:1 volume ratio). Chloroform was added dropwise in appropriate amount to completely precipitate the QDs. The vial was rapidly placed in a centrifugation apparatus and centrifuged at 4000 rpm for ~2 min.

Determination of the Concentration of QDs :

The Concentration of CdSe core QDs was calculated using the extinction coefficient reported by Peng and coworkers [32]. Core/shell QDs was synthesized through Single-Precursor Approach [23b, 30], and it was assumed that the concentration of the core/shell QDs should remain the same as the core QDs. The concentration of the raw CdSe/3CdS QDs solution is 1×10^{-5} M. The concentration of the purified CdSe/3CdS QDs solution is 2×10^{-5} M.

General procedures for imine synthesis

Synthesis of aldimines [33]:

To a solution of substituted benzaldehyde (5mmol) in dichloromethane (5mL) were slowly added aniline (6mmol). After 30 min, anhydrous magnesium sulfate (0.75 g) is added in one portion. The reaction mixture is stirred at room temperature for 2h. The resulting mixture was filtered to remove the magnesium sulfate, and the filtrate is concentrated at reduced pressure by rotary evaporation at room temperature to afford product.

Synthesis of ketimine [34]:

Benzophenone (0.91 g, 5.0 mmol) and activated molecular sieves 4A (2.0 g) were placed in a 25 mL reaction flask. A solution of aniline (0.56 g, 6 mmol) in toluene (10.0 mL) were added under argon atmosphere, and the mixture was heated under reflux overnight. After being cooled, the resulting mixture was filtered to remove the molecular sieves. The filtrate was evaporated, and the resulting pale yellow solid was recrystallized from ethanol.

*N-benzylaniline (**3a**)*. yellow liquid [colorless oil][14,35], 88% (64.5 mg). ^{1}H NMR (400 MHz, $CDCl_3$) δ7.37 – 7.32 (m, 4H), 7.30 – 7.27 (m, 1H), 7.20 – 7.16 (m, 2H), 6.74 (t, 1H, *J* = 7.2 Hz), 6.67 (d, 2H, *J* = 8.4 Hz), 4.34 (s, 2H). ^{13}C{^{1}H} NMR (100 MHz, $CDCl_3$) δ 148.2, 139.4, 129.3, 128.7, 127.6, 127.3, 117.6, 112.9, 48.4.

*4-(benzylamino)phenol (**3b**)*. brown solid, m.p. 88-90 ℃[88-90℃][36], 83% (66.2 mg). ^{1}H NMR (400 MHz, $CDCl_3$) δ 7.38 – 7.32 (m, 4H), 7.28 (d, 1H, *J* = 6.8 Hz), 6.70 (d, 2H, *J* = 8.8Hz), 6.56 (d, 2H, *J* = 8.8 Hz), 4.28 (s, 2H). ^{13}C{^{1}H} NMR (100 MHz, $CDCl_3$) δ 147.8, 142.3, 139.5, 128.6, 127.6, 127.2, 116.2, 114.4, 49.3.

*N-benzyl-4-methoxyaniline (**3c**)*. brown solid, m.p. 49-51℃[48-50℃][36], 84% (71.8 mg). ^{1}H NMR (400 MHz, $CDCl_3$) δ 7.39 – 7.32 (m, 4H), 7.28 (d, 1H, *J* = 6.8 Hz), 6.80 – 6.76 (m, 2H), 6.64 (d, 2H, *J* = 8.8 Hz), 4.29 (s, 2H), 3.74 (s, 3H). ^{13}C{^{1}H} NMR (100 MHz, $CDCl_3$) δ 152.5, 141.7, 139.2, 128.6, 127.7, 127.3, 114.8, 114.6, 55.8, 49.5.

*N-benzyl-4-fluoroaniline (**3d**)*. brown solid, m.p. 33-34 ℃ [33-35℃][37], 82% (65.8 mg). ^{1}H NMR (400 MHz, $CDCl_3$) δ 7.38 –7.29 (m, 5H), 6.92 – 6.86 (m, 2H), 6.59 – 6.56 (m, 2H), 4.30 (s, 2H), 3.90 (s, 1H). ^{13}C{^{1}H} NMR (100 MHz, $CDCl_3$) δ 155.9 (d, *J* = 234.0 Hz), 144.4, 139.2, 128.7, 127.5, 127.4, 115.7 (d, *J* = 22.0 Hz), 113.7 (d, *J* = 8.0 Hz), 48.9.

*N-benzyl-4-chloroaniline (**3e**)*. brown solid, m.p. 45-46 ℃ [46-47℃][35], 90% (78.5 mg). ^{1}H NMR (400 MHz, $CDCl_3$) δ 7.34(d, 4H, *J* = 4.4 Hz), 7.31 – 7.26 (m, 1H), 7.10 (dt, 2H, *J* = 8.8, 2.7 Hz), 6.55 (dt, 2H, *J* = 8.8, 2.6 Hz), 4.30 (s, 2H). ^{13}C{^{1}H} NMR (100 MHz, $CDCl_3$) δ 146.5, 138.8, 129.1, 128.7, 127.5, 127.4, 122.2, 114.0, 48.4.

*4-methoxy-N-(4-methylbenzyl)aniline (**3f**)*.[38] brown solid, m.p. 98-99 ℃, 93% (85 mg). ^{1}H NMR (400 MHz, $CDCl_3$) δ 7.26 (d, 2H, *J* = 8.0 Hz), 7.14 (d, 2H, *J* = 8.0 Hz), 6.77 (d, 2H, *J* = 8.8 Hz), 6.61 (dt, 2H, *J* = 8.8, 2.9 Hz), 4.23 (s, 2H), 3.74 (s, 3H), 2.34 (s, 3H). ^{13}C{^{1}H} NMR (100 MHz, $CDCl_3$) δ 152.2, 142.3, 136.9, 136.5, 129.3, 127.6, 116.4, 114.8, 114.2, 55.8, 49.0, 21.2.

*4-methyl-N-(4-methylbenzyl)aniline (**3g**)*. yellow solid, m.p. 55-56 ℃ [55-56℃][39], 88% (74.2 mg). ^{1}H NMR (400 MHz, $CDCl_3$) δ 7.26 (d, 2H, *J* = 7.6 Hz), 7.14 (d, 2H, *J* = 7.6 Hz), 6.98 (d, 2H, *J* = 8.0 Hz), 6.57 – 6.55 (m, 2H), 4.26 (s, 2H), 3.91 (s, 1H), 2.34 (s, 3H), 2.23 (s, 3H). ^{13}C{^{1}H} NMR (100 MHz, $CDCl_3$) δ 146.0, 136.8, 136.5, 129.8, 129.3, 127.5, 126.7, 113.0, 48.4, 21.2, 20.5.

*4-fluoro-N-(4-methylbenzyl)aniline (**3h**)*. [40] yellow solid, m.p. 68-70 ℃, 82% (70.5 mg). ^{1}H NMR (400 MHz, $CDCl_3$) δ 7.25 (d, 2H, *J* = 6.8 Hz), 7.15 (d, 2H, *J* = 7.6 Hz), 6.90 – 6.85 (m, 2H), 6.58 – 6.55 (m, 2H), 4.24 (s, 2H), 2.34 (s, 3H). ^{13}C{^{1}H} NMR (100 MHz, $CDCl_3$) δ 155.9 (d, *J* = 234.0 Hz), 144.4, 137.0, 136.1, 129.4, 127.5, 115.7 (d, *J* = 22.0 Hz), 113.7 (d, *J* = 7.0 Hz), 48.7, 21.2.

*4-chloro-N-(4-methylbenzyl)aniline (**3i**)*. [40] yellow solid, m.p. 65-67 ℃, 86% (79.3 mg). ^{1}H NMR (400 MHz, $CDCl_3$) δ 7.23 (d, 2H, *J* = 8.0 Hz), 7.15 – 7.10 (m, 4H), 6.60 – 6.58 (m, 2H), 4.26 (s, 2H), 2.34 (s, 3H). ^{13}C{^{1}H} NMR (100 MHz, $CDCl_3$) δ 146.7, 137.1, 135.8, 129.4, 129.1, 127.4, 122.0, 113.9, 48.1, 21.2.

*N-(4-fluorobenzyl)-4-methoxyaniline (**3j**)*.[41] brown liquid, 94% (86.6 mg). ^{1}H NMR (400 MHz, $CDCl_3$) δ 7.34 – 7.31 (m, 2H), 7.01 (t, 2H, *J* = 8.6 Hz), 6.79 – 6.75 (m, 2H), 6.60 – 6.56 (m, 2H), 4.24 (s, 2H), 3.73 (s, 3H). ^{13}C{^{1}H} NMR (100 MHz, $CDCl_3$) δ 162.0 (d, *J* = 243.0 Hz), 152.3, 142.1, 135.3, 129.1 (d, *J* = 8.0 Hz), 115.4 (d, *J* = 21.0 Hz), 114.9, 114.2, 55. 8, 48.6.

*4-fluoro-N-(4-fluorobenzyl)aniline (**3k**)*.[42] yellow solid, m.p. 49-50 ℃, 86% (75.4 mg). ^{1}H NMR (400 MHz, $CDCl_3$) δ 7.31 (t, 2H, *J* = 6.8 Hz), 7.02 (t, 2H, *J* = 8.6 Hz), 6.90 – 6.85 (m, 2H), 6.56 – 6.52 (m, 2H), 4.24 (s, 2H), 4.01 (s, 1H). ^{13}C{^{1}H} NMR (100 MHz, $CDCl_3$) δ 162.1 (d, *J* = 244.0 Hz), 156.0 (d, *J* = 234.0 Hz), 144.2, 134.8, 129.1 (d, *J* = 8.0 Hz), 115.8, 115.5 (d, *J* = 21.0 Hz), 113.8 (d, *J* = 8.0 Hz), 48.3.

*4-chloro-N-(4-fluorobenzyl)aniline (**3l**)*.[43] yellow solid, m.p. 50-52 ℃, 92% (86.7 mg). ^{1}H NMR (400 MHz, $CDCl_3$) δ 7.31 – 7.29 (m, 2H),7.11 (dt, 2H,*J* = 8.8, 2.6 Hz), 7.05 – 7.00 (m, 2H), 6.56 – 6.53 (m, 2H), 4.27 (s, 2H). ^{13}C{^{1}H} NMR (100 MHz, $CDCl_3$) δ 162.1 (d, *J* = 244.0 Hz), 146.4, 134.6 (d, *J* = 4.0 Hz), 129.1, 129.0 (d, *J* = 8.0 Hz), 122.2, 115.6 (d, *J* = 21.0 Hz), 114.0, 47.6 .

*N-(4-chlorobenzyl)-4-fluoroaniline (**3m**)*. yellow solid, m.p.123-124℃ [123.1-124.6℃][44], 81% (76.5 mg). ^{1}H NMR (400 MHz, $CDCl_3$) δ 7.32 – 7.28 (m, 4H), 6.90 – 6.86 (m, 2H), 6.56 – 6.52 (m, 2H), 4.27 (s, 2H). ^{13}C{^{1}H} NMR (100 MHz, $CDCl_3$) δ 156.0 (d, *J* = 234.0 Hz), 144.2, 137.8, 133.0, 128.8, 128.7, 115.8 (d, *J* = 23.0 Hz), 113.7 (d, *J* = 7.0 Hz), 48.2.

*N-(2-chlorobenzyl)-4-fluoroaniline (**3n**)*. yellow liquid, 88% (82.8 mg). ^{1}H NMR (400 MHz, $CDCl_3$) δ 7.41-7.37 (m, 2H), 7.26 – 7.20 (m, 2H), 6.90 – 6.86 (m, 2H), 6.58 – 6.55 (m, 2H), 4.40 (s, 2H). ^{13}C{^{1}H} NMR (100 MHz, $CDCl_3$) δ 156.0 (d, *J* = 234.0 Hz), 143.8, 136.2, 133.3, 129. 6, 129.1, 128.6, 127.0, 115.7 (d, *J* = 23.0 Hz), 114.0 (d, *J* = 8.0 Hz), 46.6.

*4-chloro-N-(4-chlorobenzyl)aniline (**3o**)*. yellow solid, m.p.65-66 ℃ [68-70℃][39], 82% (82 mg). ^{1}H NMR (400 MHz, $CDCl_3$) δ 7.32 – 7.26 (m, 4H), 7.11(dt, 2H, *J* = 8.8, 2.7 Hz), 6.53 – 6.51(m, 2H), 4.29 (s, 2H). ^{13}C{^{1}H} NMR (100 MHz, $CDCl_3$) δ 146.2, 137.4, 133.1, 129.1, 128.8, 128.6, 122.5, 114.0, 47.7.

*N-(4-methoxybenzyl)-4-methylaniline (**3p**)*.[43] yellow solid, m.p. 62-64 ℃, 86% (77.7 mg). ^{1}H NMR (400 MHz, $CDCl_3$) δ 7.28 (d, 2H, *J* = 8.8 Hz), 6.99 (d, 2H, *J* = 8.0 Hz), 6.87 (d, 2H, *J* = 8.8 Hz), 6.59 (d, 2H, *J* = 8.4 Hz), 4.23 (s, 2H), 3.80 (s, 3H), 2.24 (s, 3H). ^{13}C{^{1}H} NMR (100 MHz, $CDCl_3$) δ 158.8, 146.0, 131.6, 129.8, 128.8, 126.7, 114.0, 113.0, 55.3, 48.1, 20.4.

*4-fluoro-N-(4-methoxybenzyl)aniline (**3q**)*. yellow solid, m.p. 70-71 ℃[70-71℃][45], 93% (85.8 mg). ^{1}H NMR (400 MHz, $CDCl_3$) δ 7.28 (d, 2H, *J* = 8.8 Hz), 6.90 – 6.86 (m, 4H), 6.58 – 6.55 (m, 2H), 4.21 (s, 2H), 3.80 (s, 3H). ^{13}C{^{1}H}

NMR (100 MHz, $CDCl_3$) δ 158.8, 157.0, 144.4, 131.1, 128.8, 115.6 (d, *J* = 22.0 Hz), 114.0, 113.6 (d, *J* = 7.0 Hz), 55.3, 48.4.

*4-chloro-N-(4-methoxybenzyl)aniline (**3r**)*. yellow solid, m.p. 72-73 ℃[78-81℃][46], 82% (81.3 mg). ^{1}H NMR (400 MHz, $CDCl_3$) δ 7.27(d, 2H, *J* = 7.2 Hz), 7.11(d, 2H, *J* = 8.0 Hz), 6.88(d, 2H, *J* = 7.6 Hz), 6.56(d, 2H, *J* = 8.0 Hz), 4.22 (s, 2H), 3.80 (s, 3H). ^{13}C{^{1}H} NMR (100 MHz, $CDCl_3$) δ 159.0, 146.5, 130.8, 129.0, 128.8, 122.2, 114.1, 114.0, 55.3, 47.9.

*1-(4-((4-methoxybenzyl)amino)phenyl)ethan-1-one (**3s**)*. yellow solid, m.p. 124-125 ℃[116-117][47], 68% (69.4 mg). ^{1}H NMR (400 MHz, $CDCl_3$) δ 7.84 – 7.82 (m, 2H), 7.27 (d, 2H, *J* = 6.8 Hz), 6.90 – 6.88 (m, 2H), 6.64 (d, 2H, *J* = 8.4 Hz), 4.33 (s, 2H), 3.80 (s, 3H), 2.50 (s, 3H). ^{13}C{^{1}H} NMR (100 MHz, $CDCl_3$) δ 196.5, 159.0, 152.0, 130.8, 130.1, 128.8, 126.8, 114.2, 111.6, 55.3, 47.1, 26.1.

*4-((4-cyanobenzyl)amino)benzonitrile (**3t**)*. yellow solid, m.p. 148-150 ℃, 40% (37.4 mg). ^{1}H NMR (400 MHz, $CDCl_3$) δ 7.66 – 7.64 (m, 2H), 7.45 – 7.41 (m, 4H), 6.57 – 6.55 (m, 2H), 4.49 (s, 2H). ^{13}C{^{1}H} NMR (100 MHz, $CDCl_3$) δ 150.5, 143.5, 133.9, 132.7, 127.6, 120.1, 118.6, 112.6, 111.5, 100.0, 47.0.

*N-(4-(benzyloxy)benzyl)-4-fluoroaniline (**3u**)*. yellow solid, m.p. 82-83 ℃, 85% (105 mg). ^{1}H NMR (400 MHz, $CDCl_3$) δ 7.44 – 7.35 (m, 4H), 7.34 – 7.31 (m, 1H), 7.28 (d, 2H, *J* = 8.4 Hz), 6.95 (d, 2H, *J* = 8.4 Hz), 6.91 – 6.87 (m, 2H), 6.60 – 6.59 (m, 2H), 5.06 (s, 2H), 4.21 (s, 2H). ^{13}C{^{1}H} NMR (100 MHz, $CDCl_3$) δ 158.1, 155.9 (d, *J* = 234.0 Hz), 144.3, 136.9, 131.3, 128.9, 128.6, 128.0, 127.5, 115.7 (d, *J* = 22.0 Hz), 115.0, 113.8 (d, *J* = 7.0 Hz), 70.0, 48.5.

*N-(4-fluorobenzyl)-3,4-dimethylaniline (**3v**)*. brown liquid, 90% (82.9 mg). ^{1}H NMR (400 MHz, $CDCl_3$) δ 7.34 – 7.31 (m, 2H), 7.03 – 6.99 (m, 2H), 6.93 (d, 1H, *J* = 8.0 Hz), 6.47 (d, 1H, *J* = 2.4 Hz), 6.39 (dd, 1H, *J* = 8.0, 2.4 Hz), 4.27 (s, 2H), 2.18 (s, 3H), 2.15 (s, 3H). ^{13}C{^{1}H} NMR (100 MHz, $CDCl_3$) δ 162.0 (d, *J* = 243.0 Hz), 146.1, 137.4, 135.4, 130.3, 129.0 (d, *J* = 8.0 Hz), 125.8, 115.4 (d, *J* = 22.0 Hz), 114.8, 110.3, 48.0, 20.1, 18.7.

*4-((4-(hexyloxy)benzyl)amino)benzonitrile (**3w**)*. white solid, m.p. 63-65 ℃, 85% (104.7 mg). IR (KBr) ν 3354, 3039, 2213, 1888, 1761, 1603,1516,1469, 1246, 826 cm^{-1}; ^{1}H NMR (400 MHz, $CDCl_3$) δ 7.42 (d, 2H, *J* = 8.8 Hz), 7.23 (d, 2H, *J* = 8.4 Hz), 6.88 (d, 2H, *J* = 8.4 Hz), 6.61 (d, 2H, *J* = 8.0 Hz), 4.28 (s, 2H), 3.94 (t, 2H, *J* = 6.4 Hz), 1.81 – 1.74 (m, 2H), 1.47 – 1.43 (m, 2H), 1.35 – 1.32 (m, 4H), 0.92 – 0.89 (m, 3H). ^{13}C{^{1}H} NMR (100 MHz, $CDCl_3$) δ 158.8, 133.7, 128.8, 114.8, 68.1, 31.6, 29.2, 25.7, 22.6, 14.0. HRMS (ESI-TOF)m/z: $[M+H]^+$ Calcd for $C_{20}H_{24}N_2O$ 309.1967; found 309.1954.

4-fluoro-N-(4-(trifluoromethyl)benzyl)aniline (3x). yellow solid, m.p. 90-91 ℃, 82% (88.3 mg). ^{1}H NMR (400 MHz, $CDCl_3$) δ 7.60 (d, 2H, *J* = 8.4 Hz), 7.48 (d, 2H, *J* = 8.0 Hz), 6.90 – 6.86 (m, 2H), 6.56 – 6.52(m, 2H), 4.38 (s, 2H). ^{13}C{^{1}H} NMR (100 MHz, $CDCl_3$) δ 156.2 (d, *J* = 235.0 Hz), 143.6, 143.2, 129.6 (d, J = 32.0 Hz), 127.8, 127.7, 127.6, 125.6 (q, *J* = 3.7Hz), 115.9, 115.7, 114.1, 114.0, 48.6.

*4-methoxy-N-(4-methoxybenzyl)aniline (**3y**)*. yellow solid, m.p. 94-96 ℃ [92-94℃][36], 87% (84.7 mg). ^{1}H NMR (400 MHz, $CDCl_3$) δ 7.29 (d, 2H, *J* = 8.8 Hz), 6.86 (d, 2H, *J* = 8.4 Hz), 6.78 (d, 2H, *J* = 8.8 Hz), 6.68(d, 2H, *J* = 8.4 Hz), 4.21 (s, 2H), 3.80 (s, 3H), 3.75 (s, 3H). ^{13}C{^{1}H} NMR (100MHz, $CDCl_3$) δ 158.8, 152.2, 142.3, 131.5, 128.9, 114.9, 114.3, 114.0, 55.8, 55.3, 48.8.

*N^1,N^4-bis(4-fluorobenzyl)benzene-1,4-diamine (**4**)*. brown black solid, m.p. 115-116 ℃ [115-116℃][48], 72% (93 mg). ^{1}H NMR (400 MHz, $CDCl_3$) δ 7.32 (dd, 4H, *J* = 8.4, 5.6 Hz), 7.00 (t, 4H, *J* = 8.5 Hz), 6.57 (s, 4H), 4.23 (s, 4H). ^{13}C{^{1}H} NMR (100 MHz, $CDCl_3$) δ 162.0 (d, *J* = 243.0 Hz), 140.6, 135.6 (d, *J* = 3.0 Hz), 129.1 (d, *J* = 7.0 Hz), 115.3 (d, *J* = 21.0 Hz), 114.7, 48.8.

*(4-Fluoro-benzyl)-octyl-amine (**5**)*. yellow liquid, 85% (80.7 mg). ^{1}H NMR (400 MHz, $CDCl_3$) δ 7.31 – 7.27 (m, 2H), 7.03 – 6.98 (m, 2H), 3.76 (s, 2H), 2.61 (t, 2H, *J* = 7.2 Hz), 1.54 – 1.47 (m, 2H), 1.27 (d, 10H, *J* = 4.4 Hz), 0.88 (t, 3H, *J* = 7.0 Hz). ^{13}C{^{1}H} NMR (100 MHz, $CDCl_3$) δ 161.9 (d, *J* = 243.0 Hz), 136.1 (d, *J* = 3.0 Hz), 129.6 (d, *J* = 8.0 Hz), 115.1 (d, *J* = 21.0 Hz), 53.3, 49.4, 31.8, 30.0, 29.5, 29.2, 27.3, 22.6, 14.1.

*Benzyl-cyclohexyl-amine (**6**)*. yellow liquid[yellow oil][44], 56% (42.8 mg). ^{1}H NMR (400 MHz, $CDCl_3$) δ 7.30 (d, 4H, *J* = 12.8 Hz), 7.25 – 7.23 (m, 1H), 3.80 (s, 2H), 2.52 – 2.45 (m, 1H), 1.92 – 1.90 (m, 2H), 1.75 – 1.72 (m, 2H), 1.62 – 1.61 (m, 1H), 1.30 – 1.26 (m, 2H), 1.23 – 1.17 (m, 3H). ^{13}C{^{1}H} NMR (100 MHz, $CDCl_3$) δ 140.9, 128.4, 128.1, 126.8, 56.2, 51.0, 33.5, 26.2, 25.0.

*4-fluoro-N-(1-(p-tolyl)ethyl)aniline (**7a**)*. yellow liquid, 91% (83.7 mg). ^{1}H NMR (400 MHz, $CDCl_3$) δ 7.22 (d, 2H, *J* = 8.4 Hz), 7.12 (d, 2H, *J* = 8.0 Hz), 6.80 – 6.76 (m, 2H), 6.45 – 6.41(m, 2H), 4.38 (q, 1H, *J* = 6.8 Hz), 2.31 (s, 3H), 1.48 (d, 3H, *J* = 6.4 Hz). ^{13}C{^{1}H} NMR (100 MHz, $CDCl_3$) δ 155.7 (d, *J* = 234.0 Hz), 143.5, 141.9, 136.6, 129.4, 125.8, 115.5 (d, *J* = 22.0 Hz), 114.2 (d, *J* = 7.0 Hz), 53.9, 25.1, 21.1.

*4-fluoro-N-(1-(4-fluorophenyl)ethyl)aniline (**7b**)*. yellow liquid, 83% (86.8 mg). ^{1}H NMR (400 MHz, $CDCl_3$) δ 7.32 – 7.29 (m, 2H), 7.02 – 6.98 (m, 2H), 6.82 – 6.77 (m, 2H), 6.43 – 6.40 (m, 2H), 4.39 (q, 1H, *J* = 6.8 Hz), 1.49 (d, 3H, *J* = 6.8 Hz). ^{13}C{^{1}H} NMR (100MHz, $CDCl_3$) δ 161.8 (d, *J* = 243.0 Hz), 155.8 (d, *J* = 233.0 Hz), 143.2, 140.5, 127.4, 127.3, 115.7, 115.6, 115.4, 115.4, 114.4, 114.3, 53.7, 25.1.

*N-(1-(4-chlorophenyl)ethyl)-4-fluoroaniline (**7c**)*. yellow liquid, 94% (94.3 mg). ^{1}H NMR (400 MHz, $CDCl_3$) δ 7.28 (s, 4H), 6.82 – 6.76 (m, 2H), 6.42 – 6.37 (m, 2H), 4.37 (q, 1H, *J* = 6.6 Hz), 1.47 (d, 3H, *J* = 6.8 Hz). ^{13}C{^{1}H} NMR (100 MHz, $CDCl_3$) δ 155.8 (d, *J* = 234.0 Hz), 143.6, 143.2, 132.5, 129.8, 128.8, 127.2, 115.7, 115.5, 114.2, 114.1, 53.6, 25.1.

*N-(4-fluorobenzyl)-1-phenylethan-1-amine (**8**)*.[49] yellow liquid, 63% (57.8 mg). ^{1}H NMR (400 MHz, $CDCl_3$) δ 7.35 – 7.33 (m, 4H), 7.28 – 7.26 (m, 1H), 7.25 – 7.22 (m, 2H), 7.01 – 6.96 (m, 2H), 3.79 (q, 1H, *J* = 6.6 Hz), 3.59 (q, 2H, *J* = 13.1 Hz), 1.37 (d, 3H, *J* = 6.4 Hz). ^{13}C{^{1}H} NMR (100 MHz, $CDCl_3$) δ 161.9 (d, *J* = 243.0 Hz), 145.2, 136.0, 129.8, 129.7, 128.5, 127.1, 126.7, 115.2, 115.0, 57.5, 50.8, 24.4.

*Benzhydryl-phenyl-amine (**9**)*. yellow oil [yellow oil][13], 67% (69.8 mg). ^{1}H NMR (400 MHz, $CDCl_3$) δ 7.34 – 7.30 (m, 8H), 7.27 – 7.24 (m, 3H), 6.84 – 6.79 (m, 2H), 6.48 – 6.46 (m, 2H), 5.42 (s, 1H). ^{13}C{^{1}H} NMR (100 MHz, $CDCl_3$) δ 142.8, 128.8, 127.4, 127.4, 115.6, 115.4, 114.3,114.3, 63.6.*Butenafine (**10**)*. yellow liquid [200-202℃][50], 65% (82.5mg). ^{1}H NMR (400 MHz, $CDCl_3$) δ 8.22 – 8.21 (m, 1H), 7.84 – 7.82 (m, 1H), 7.76 (d, 1H, J = 8.0 Hz), 7.50 – 7.44 (m, 3H), 7.41 – 7.38 (m, 1H), 7.35 – 7.29 (m, 2H), 7.28 (d, 2H, J = 8.4 Hz), 3.93 (s, 2H), 3.58 (s, 2H), 2.20 (s, 3H), 1.31 (s, 9H). ^{13}C{^{1}H} NMR (100 MHz, $CDCl_3$) δ 149.9, 136.2, 135.0, 133.9, 132.5, 128.8, 128.4, 127.9, 127.4, 125.7, 125.6, 125.1, 124.9, 62.0, 60.4, 42.4, 34.5, 31.4.

ASSOCIATED CONTENT

AUTHOR INFORMATION

Corresponding Author

*E-mail:shenym@zstu.edu.cn (Y.-M. Shen).

*E-mail: puchaodan@zju.edu.cn (C.-D. Pu).

ORCID

Yong-Miao Shen: 0000-0002-9382-9744

Author Contributions

†Zi-Wei Xi and Lei Yang contributed equally to this work.

Notes

The authors declare no competing financial interest.

ACKNOWLEDGMENT

This work was supported by the National Natural Science Foundation of China (NSFC 21202101), Zhejiang Provincial Natural Science Foundation of China (LY16B020006) and China Postdoctoral Science Foundation (2015M581919 and 2016M601930).

SUPPORTING INFORMATION

Additional experimental details and NMR spectra for obtained compounds (PDF)

The Supporting Information is available free of charge on the ACS Publications website.

REFERENCES

(1) Lawrence, S. A. Amines: Synthesis, properties and applications, *Cambridge University Press*. **2004**.

(2) For reviews on transition metal complexes catalyzed hydrogenations and transfer hydrogenations, see (a) Li, W.; Zhang, X. Asymmetric hydrogenation of imines. In Stereoselective Formation of Amines. *Top Curr. Chem.* **2014,** *343*, 103–144. (b) Verendel, J. J.; Pàmies, O.; Diéguez, M.; Andersson, P. G. Asymmetric hydrogenation of olefins using chiral crabtree-type catalysts: Scope and limitations. *Chem. Rev.* **2014,** *114*, 2130–2169. (c) Etayo, P.; Vidal-Ferran, A. Rhodium-catalysed asymmetric hydrogenation as a valuable synthetic tool for the preparation of chiral drugs. *Chem. Soc. Rev.* **2013,** *42*, 728–754. (d) Ager, D. J.; de Vries, A. H. M.; de Vries, J. G. Asymmetric homogeneous hydrogenations at scale. *Chem. Soc. Rev.* **2012,** *41*,

3340–3380. (e) Xie, J.-H.; Zhu, S.-F.; Zhou, Q.-L. Transition metal-catalyzed enantioselective hydrogenation of enamines and imines. *Chem. Rev.* **2011,** *111,* 1713–1760.

(3) For reviews on organo–Brønsted acids for transfer hydrogenation of imines with Hantzsch esters, see (a) Faisca Phillips, A. M.; Pombeiro, A. J. L. Recent advances in organocatalytic enantioselective transfer hydrogenation. *Org. Biomol. Chem.* **2017,** *15,* 2307−2340. (b) Zheng, C.; You, S. L. Transfer hydrogenation with Hantzsch esters and related organic hydride donors. *Chem. Soc. Rev.* **2012,** *41,* 2498−2518. (c) Rueping, M.; Dufour, J.; Schoepke, F.R. Advances in catalytic metal-free reductions: from bio-inspired concepts to applications in the organocatalytic synthesis of pharmaceuticals and natural products. *Green Chem.* **2011,** *13,* 1084–1105.

(4) For reviews on metal–organo cooperative catalytic hydrogenations, see (a) Tang, W.; Xiao, J. Asymmetric hydrogenation of imines via metal–organo cooperative catalysis. *Synthesis* **2014,** *46,* 1297–1302. (b) Du, Z.; Shao, Z. Combining transition metal catalysis and organocatalysis–an update. *Chem. Soc. Rev.* **2013,** *42,* 1337–1378. (c) Stegbauer, L.; Sladojevich, F.; Dixon, D. J. Bifunctional organo/metal cooperative catalysis with cinchona alkaloid scaffolds. *Chem. Sci.* **2012,** *3,* 942–958.

(5) For selected recent reviews, see (a) Matsui, J. K.; Lang, S. B.; Heitz, D. R.; Molander, G. A. Photoredox-mediated routes to radicals: The value of catalytic radical generation in synthetic methods development. *ACS Catal.* **2017,** *7,* 2563–2575. (b) Romero, N. A.; Nicewicz, D. A. Organic photoredox catalysis. *Chem. Rev.* **2016,** *116,* 10075–10166. (c) Shaw, M. H.; Twilton, J.; MacMillan, D. W. Photoredox catalysis in organic chemistry. *J. Org. Chem.* **2016,** *81,* 6898–6926. (d) Schultz, D. M.; Yoon, T. P. Solar synthesis: prospects in visible light photocatalysis. *Science.* **2014,** *343,* 1239176. (e) Prier, C. K.; Rankic, D. A.; MacMillan, D. W. C. Visible light photoredox catalysis with transition metal complexes: applications in organic synthesis. *Chem. Rev.* **2013,** *113,* 5322–5363. (f) Xuan, J.; Xiao, W.-J. Visible–light photoredox catalysis. *Angew. Chem., Int. Ed.* **2012,** *51,* 6828–6838. (g) Narayanam, J. M. R.; Stephenson, C. R. J. Visible light photoredox catalysis: applications in organic synthesis. *Chem. Soc. Rev.* **2011,** *40,* 102–113.

(6) (a) Hari, D. P.; König, B. Synthetic applications of eosin Y in photoredox catalysis. *Chem. Commun.* **2014,** *50,* 6688–6699. (b) Fukuzumi, S.; Ohkubo, K. Organic synthetic transformations using organic dyes as photoredox catalysts. *Org. Biomol. Chem.* **2014,** *12,* 6059–6071.

(7) (a) Hager, D.; MacMillan, D. W. Activation of C–H bonds via the merger of photoredox and organocatalysis: a coupling of benzylic ethers with Schiff bases. *J. Am. Chem. Soc.* **2014,** *136,* 16986–16989. (b) Jeffrey, J. L.; Petronijevic, F. R.; MacMillan, D. W. Selective radical–radical cross-couplings: design of a formal β-mannich reaction. *J. Am. Chem. Soc.* **2015,** *137,* 8404–8407. (c) Patel, N. R.; Kelly, C. B.; Siegenfeld, A. P.; Molander, G. A. Mild, redox-neutral alkylation of imines enabled by an organic photocatalyst. *ACS Catal.* **2017,** *7,* 1766–1770. (d) Lee, K. N.; Lei, Z.; Ngai, M.-Y. β-Selective reductive coupling of alkenylpyridines with aldehydes and imines via synergistic lewis acid/photoredox catalysis. *J. Am. Chem. Soc.* **2017,** *139,* 5003–5006. (e) Zhang, H.-H.; Yu, S. Radical alkylation of imines with 4-alkyl-1, 4-dihydropyridines enabled by photoredox/brønsted acid cocatalysis. *J. Org. Chem.* **2017,** *82,* 9995−10006.

(8) (a) Qi, L.; Chen, Y. Polarity–reversed allylations of aldehydes, ketones, and imines enabled by Hantzsch ester in photoredox catalysis. *Angew. Chem., Int. Ed.* **2016,** *55,* 13312–13509. (b) Fuentes de Arriba, A. L.; Urbitsch, F.; Dixon, D. J. Umpolung synthesis of branched α-functionalized amines from imines via photocatalytic three-component reductive coupling reactions. *Chem. Commun.* **2016,** *52,* 14434−14437. (c) Jeffrey, J. L.; Petronijević, F. R.; MacMillan, D. W. C. Selective radical–radical cross-couplings: design of a formal β-mannich reaction. *J. Am. Chem. Soc.* **2015,** *137,* 8404−8407.

(9) (a) Uraguchi, D.; Kinoshita, N.; Kizu, T.; Ooi, T. J. Am. *Chem. Soc.* **2015,** *137,* 13768−13771. (b) Kizu, T.; Uraguchi, D.; Ooi, T. Independence from the sequence of single-electron transfer of photoredox process in redox-neutral asymmetric bond-forming reaction. *J. Org. Chem.* **2016,** *81,* 6953−6958. (c) Fava, E.; Millet, A.; Nakajima, M.; Loescher, S.; Rueping, M. Reductive umpolung of carbonyl derivatives with visible-light photoredox catalysis: Direct access to vicinal diamines and amino alcohols via α - amino radicals and ketyl radicals. *Angew. Chem., Int. Ed.* **2016,** *55,* 6776–6779.

(10) Chen, M.; Zhao, X.; Yang, C.; Xia, W. Visible-light-triggered directly reductive arylation of carbonyl/iminyl derivatives through photocatalytic PCET. *Org. Lett.* **2017,** *19,* 3807–3810.

(11) (a) Nakajima, M.; Fava, E.; Loescher, S.; Jiang, Z.; Rueping, M. Photoredox-catalyzed reductive coupling of aldehydes, ketones, and imines with visible light. *Angew. Chem., Int. Ed.* **2015,** *54,* 8828–8832. (b) Okamoto, S.; Kojiyama, K.; Tsujioka, H.; Sudo, A. Metal-free reductive coupling of C= O and C= N bonds driven by visible light: use of perylene as a simple photoredox catalyst. *Chem. Commun.* **2016,** *52,* 11339–11342. (c) Okamoto, S.; Ariki, R.; Tsujioka, H.; Sudo, A. A metal-free approach to 1, 2-diamines via visible light-driven reductive coupling of imines with perylene as a photoredox catalyst. *J. Org. Chem.* **2017,** *82,* 9731–9736.

(12) Zhou, N.; Yuan, X. A.; Zhao, Y.; Xie, J.; Zhu, C. Synergistic photoredox catalysis and organocatalysis for inverse hydroboration of imines. *Angew. Chem., Int. Ed.* **2018,** *57,* 4054–4058.

(13) (a) Jiang, H,; Bellomo, A.; Zhang, M.; Carroll, P. J.; Manor, B. C.; Jia, T.; Walsh, P. J. Visible-light-mediated umpolung reactivity of imines: Ketimine reductions with Cy_2NMe and water. *Org. Lett.* **2018,** *20,* 2433−2436. (b) Van As, D. J.; Connell, T. U.; Brzozowski, M.; Scully, A. D.; Polyzos, A. Photocatalytic and chemoselective transfer hydrogenation of diarylimines in batch and continuous flow. *Org. Lett.* **2018,** *20,* 905−908. (c) Guo, X.; Okamoto, Y.; Schreier, M. R.; Ward, T. R.; Wenger, O. S. Enantioselective synthesis of amines by combining photoredox and enzymatic catalysis in a cyclic reaction network. *Chem. Sci.* **2018,** *9,* 5052-5056.

(14) (a) Alam, R.; Molander, G. A. Photoredox-catalyzed direct reductive amination of aldehydes without an external hydrogen/hydride source. *Org. Lett.* **2018,** *20,* 2680−2684. (b) Guo, X.; Wenger, O. S. Reductive amination by photoredox catalysis and polarity‐matched hydrogen atom transfer. *Angew. Chem., Int. Ed.* **2018,** *57,* 2469−2473.

(15) (a) Weiss, E. A. Designing the surfaces of semiconductor quantum dots for colloidal photocatalysis. *ACS Energy Lett.* **2017,** *2,* 1005−1013. (b) Wang, R.; Lu, K.-Q.; Tang, Z.-R.; Xu, Y.-J. Recent progress in carbon quantum dots: synthesis, properties and applications in photocatalysis. *J. Mater. Chem. A* **2017,** *5,* 3717−3734.

(16) (a) Sahai, S.; Ikram, A.; Rai, S.; Shrivastav, R.; Dass, S.; Satsangi, V. R. Quantum dots sensitization for photoelectrochemical generation of hydrogen: A review. *Renew. Sust. Energ. Rev.* **2017,** *68,* 19−27. (b) Mohmood, I.; Lopes, C.B.; Lopes, I.; Ahmad, I.; Duarte, A.C.; Pereira, E. Nanoscale materials and their use in water contaminants removal-a review. *Environ. Sci. Pollut. Res.* **2013,** *20,* 1239–1260. (c) Li, X. B.; Li, Z. J.; Gao, Y. J.; Meng, Q. Y.; Yu, S.; Weiss, R. G.; Tung, C. H.; Wu, L. Z. Mechanistic insights into the interface-directed transformation of thiols into disulfides and molecular hydrogen by visible–light irradiation of quantum dots. *Angew. Chem. Int. Ed.* **2014,** *53,* 2085–2089. (d) Aldana, J.; Wang, Y. A.; Peng, X. Photochemical instability of CdSe nanocrystals coated by hydrophilic thiols. *J. Am. Chem. Soc.* **2001,** *123,* 8844–8850.

(17) (a) Warrier, M.; Lo, M. K. F.; Monbouquette, H.; Garcia-Garibay, M. A. Photocatalytic reduction of aromatic azides to amines using CdS and CdSe nanoparticles. *Photochem. Photobiol. Sci.* **2004,** *3,* 859–863. (b) Chauviré, T.; Mouesca, J.-M.; Gasparutto, D.; Ravanat, J.-L.; Lebrun, C.; Gromova, M.; Jouneau, P.-H.; Chauvin, J.; Gambarelli, S.; Maurel, V. Redox photocatalysis with water-soluble core-shell CdSe-ZnS quantum dots. *J. Phys. Chem. C* **2015,** *119,* 17857–17866. (c) Jensen, S. C.; Homan, S. B.; Weiss, E. A. Photocatalytic conversion of nitrobenzene to aniline through sequential proton-coupled one-electron transfers from a cadmium sulfide quantum dot. *J. Am. Chem. Soc.* **2016,** *138,* 1591–1600.

(18) Pal, A.; Ghosh, I.; Sapra, S.; König, B. Quantum dots in visible-light photoredox catalysis: Reductive dehalogenations and C–H arylation reactions using aryl bromides. *Chem. Mater.* **2017,** *29,* 5225−5231.

(19) (a) Caputo, J. A.; Frenette, L. C.; Zhao, N.; Sowers, K. L.; Krauss, T. D.; Weix, D. J. General and efficient C–C bond forming photoredox catalysis with semiconductor quantum dots. *J. Am. Chem. Soc.* **2017,** *139,* 4250−4253. (b) Zhang, Z.; Edme, K.; Lian, S.; Weiss, E. A. Enhancing the rate of quantum-dot-photocatalyzed carbon–carbon Coupling by tuning the composition of the dot's ligand shell. *J. Am. Chem. Soc.* **2017,** *139,* 4246−4249.

(20) (a) Kisch, H. Semiconductor photocatalysis for chemoselective radical coupling reactions. *Acc. Chem. Res.* **2017**, *50,* 1002−1010. (b) Shiraishi, Y.; Fujiwara, K.; Sugano, Y.; Ichikawa, S.; Hirai, T. N-Monoalkylation of amines with alcohols by

tandem photocatalytic and catalytic reactions on TiO_2 loaded with Pd nanoparticles. *ACS Catal.* **2013**, *3*, 312−320. (c) Schindler, W.; Knoch, F.; Kisch, H. Semiconductor-catalysed photoaddition: γ, δ-Unsaturated amines from cyclopentene and Schiff bases. *Chem. Ber.* **1996**, *129*, 925−932.

(21) (a) Zhu, H.; Song, N.; Lian, T. Controlling charge separation and recombination rates in CdSe/ZnS type I core− shell quantum dots by shell thicknesses. *J. Am. Chem. Soc.* **2010,** *132*, 15038−15045. (b) Qiu, F.; Han, Z.; Peterson, J. J.; Odoi, M. Y.; Sowers, K. L.; Krauss, T. D. Photocatalytic hydrogen generation by CdSe/CdS nanoparticles. *Nano Lett.* **2016,** *16*, 5347−5352.

(22) (a) Zhao, J.; Holmes, M. A.; Osterloh, F. E. Quantum confinement controls photocatalysis: a free energy analysis for photocatalytic proton reduction at CdSe nanocrystals. *ACS nano* **2013,** *7*, 4316−4325. (b) Kuehnel, M. F.; Wakerley, D. W.; Orchard, K. L.; Reisner, E. Photocatalytic formic acid conversion on CdS nanocrystals with controllable selectivity for H_2 or CO. *Angew. Chem. Int. Ed.* **2015,** *54*, 9627−9631.

(23) (a) Zhou, J.; Zhu, M.; Meng, R.; Qin, H.; Peng, X. Ideal CdSe/CdS core/shell nanocrystals enabled by entropic ligands and their core size-, shell thickness-, and ligand-dependent photoluminescence properties. *J. Am. Chem. Soc.* **2017,** *139*, 16556–16567. (b) Pu, C.; Peng, X. To battle surface traps on CdSe/CdS core/shell nanocrystals: shell isolation versus surface treatment. *J. Am. Chem. Soc.* **2016,** *138*, 8134–8142. (c) Niu, Y.; Pu, C.; Lai, R.; Meng, R.; Lin, W.; Qin, H.; Peng, X. One-pot/three-step synthesis of zinc-blende CdSe/CdS core/shell nanocrystals with thick shells. *Nano Res.* **2017,** *10*, 1149–1162. (d) Yang, Y.; Li, J.; Lin, L.; Peng, X. An efficient and surface-benign purification scheme for colloidal nanocrystals based on quantitative assessment. *Nano Res.* **2015,** *8*, 3353–3364. (e) Yu, W. W.; Peng, X. Formation of high-quality CdS and other II-VI semiconductor nanocrystals in noncoordinating solvents: tunable reactivity of monomers. *Angew. Chem., Int. Ed.* **2002**, *41*, 2368–2371.

(24) Bordwell, F. G. Equilibrium acidities in dimethyl sulfoxide solution. *Acc. Chem. Res.* **1988**, *21*, 456−463.

(25) (a) Bordwell, F. G.; Zhang, X.-M.; Satish, A. V.; Cheng, J.-P. Assessment of the importance of changes in ground-state energies on the bond dissociation enthalpies of the OH bonds in phenols and the SH bonds in thiophenols. *J. Am. Chem. Soc.* **1994,** *116*, 6605–6610. (b) Ogawa, K. A.; Boydston, A. J. Organocatalyzed anodic oxidation of aldehydes to thioesters. *Org. Lett.* **2014**, *16*, 1928−1931.

(26) Kisch, H. Semiconductor photocatalysis-mechanistic and synthetic aspects. *Angew. Chem. Int. Ed.* **2013,** *52*, 812–847.

(27) (a) Morris-Cohen, A. J.; Frederick, M. T.; Cass, L. C.; Weiss, E. A. Simultaneous determination of the adsorption constant and the photoinduced electron transfer rate for a CdS quantum dot−viologen complex. *J. Am. Chem. Soc.* **2011,** *133*, 10146–10154. (b) Robel, I.; Kuno, M.; Kamat, P. V. Size-dependent electron injection from excited CdSe quantum dots into TiO_2 nanoparticles. *J. Am. Chem. Soc.* **2007,** *129*, 4136–4137. (c) Zhu, H.; Song, N.; Rodr ́guez C ́ordoba, W.; Lian, T. Wave function engineering for efficient extraction of up to nineteen electrons from one CdSe/CdS quasi-type II quantum dot. *J. Am. Chem. Soc.* **2012,** *9*, 4250–4257. (d) Zhu, H.; Yang, Y.; Hyeon-Deuk, K.; Califano, M.; Song, N.; Wang, Y.; Zhang, W.; Prezhdo, O. V.; Lian, T. Auger-assisted electron transfer from photoexcited semiconductor quantum dots. *Nano Lett.* **2014,** *14*, 1263–1269.

(28) Zhu, X.-Q.; Liu, Q.-Y.; Chen, Q.; Mei, L.-R. Hydride, hydrogen, proton, and electron affinities of imines and their reaction intermediates in acetonitrile and construction of thermodynamic characteristic graphs (TCGs) of imines as a "Molecule ID Card". *J. Org. Chem.* **2010,** *75*, 789–808.

(29) Thomson, J. W.; Nagashima, K.; Macdonald, P. M.; Ozin, G. A. From sulfur− amine solutions to metal sulfide nanocrystals: peering into the oleylamine− sulfur black box. *J. Am. Chem. Soc.* **2011,** *133*, 5036–5041.

(30) Niu, Y.; Pu, C.; Lai, R.; Meng, R.; Lin, W.; Qin, H.; Peng, X. One-pot/three-step synthesis of zinc-blende CdSe/CdS core/shell nanocrystals with thick shells. *Nano Res.* **2017,** *10*, 1149–1162.

(31) Yang, Y.; Li, J.; Lin, L.; Peng, X. An efficient and surface-benign purification scheme for colloidal nanocrystals based on quantitative assessment. *Nano Res.* **2015,** *8*, 3353–3364.

(32) Li, J.; Chen, J.; Shen, Y.; Peng, X. Extinction coefficient per CdE (E = Se or S) unit for zinc-blende CdE nanocrystals. *Nano Res.* **2018,** *11*, 3991–4004.

(33) Danheiser, R. L., Okamoto, I.; Lawlor, M. D.; Lee, T. W. Generation and [2+ 2] cycloadditions of thio-substituted ketenes: trans-1-(4-methoxyphenyl)-4-phenyl-3-(phenylthio) azetidin-2-one: (2-azetidinone, 1-(4-methoxyphenyl)-4-phenyl-3-(phenylthio)-, trans-). *Org. synth.* **2003,** 160–171.

(34) Hayashi, S.; Yorimitsu, H.; Oshima, K. Synthesis of aziridines by palladium-catalyzed reactions of allylamines with aryl and alkenyl halides: Evidence of a syn-carboamination pathway. *Angew. Chem. Int. Ed.*, **2009,** *48,* 7224–7226.

(35) Zhu, X.; Su, L.; Huang, L.; Chen, G.; Wang, J.; Song, H.; Wan, Y. A facile and efficient oxalyldihydrazide/ketone-promoted copper-catalyzed amination of aryl halides in water. *Eur. J. Org. Chem.* **2009,** 635─642.

(36) Huang, Y. B.; Yi, W. B.; Cai, C. An efficient, recoverable fluorous organocatalyst for direct reductive amination of aldehydes. *J. Fluorine Chem.* **2010,** *131*, 879─882.

(37) Garibotto, F. M.; Sortino, M. A.; Kouznetsov, V. V.; Enriz, R. D.; Zacchino, S. A. Synthesis and antifungal activity of N-aryl-N-benzylamines and of their homoallyl analogues. *ARKIVOC.* **2011,** 149─161.

(38) Jagadeesh, R. V.; Murugesan, K.; Alshammari, A. S.; Neumann, H.; Pohl, M. M.; Radnik, J.; Beller, M. MOF-derived cobalt nanoparticles catalyze a general synthesis of amines. *Science.* **2017,** *358*, 326─332.

(39) Anil Kumar, K.; Sreelekha, T. S.; Shivakumara, K. N.; Prakasha, K. C.; Gowda, D. C. Zinc-catalyzed reduction of imines by triethylsilane. *Synth. Commun*. **2009,** *39*, 1332─1341.

(40) Xu, Z.; Wang, D. S.; Yu, X.; Yang, Y.; Wang, D. Tunable triazole-phosphine-copper catalysts for the synthesis of 2-aryl-1H-benzo [d] imidazoles from benzyl alcohols and diamines by acceptorless dehydrogenation and borrowing hydrogen reactions. *Adv. Synth. Catal.* **2017,** *359*, 3332─3340.

(41) Arachchige, P. T. K.; Lee, H.; Yi, C. S. Synthesis of symmetric and unsymmetric secondary amines from the ligand-promoted ruthenium-catalyzed deaminative coupling reaction of primary amines. *J. Org. Chem*. **2018,** *83*, 4932─4947.

(42) Wei, Y.; Zhao, C.; Xuan, Q.; Song, Q. An expedient and novel strategy for reductive amination by employing H_2O as both a hydrogen source and solvent via $B_2(OH)_4/H_2O$ systems. *Org. Chem. Fronti.* **2017,** *4*, 2291─2295.

(43) Prakash, G. S.; Do, C.; Mathew, T.; Olah, G. A. Gallium (III) triflate catalyzed direct reductive amination of aldhydes. *Catal. Let.* **2010,** *137*, 111─117.

(44) Liao, W.; Chen, Y.; Liu, Y.; Duan, H.; Petersen, J. L.; Shi, X. 1, 2, 3-Triazole-boranes: stable and efficient reagents for ketone and aldehyde reductive amination in organic solvents or in water. *Chem. Commun*. **2009,** 6436─6438.

(45) Sousa, S. C.; Fernandes, A. C. Efficient and highly chemoselective direct reductive amination of aldehydes using the system silane/oxorhenium complexes. *Adv. Synth. Catal.* **2010,** *352*, 2218─2226.

(46) Reddy, P. S.; Kanjilal, S.; Sunitha, S.; Prasad, R. B. Reductive amination of carbonyl compounds using $NaBH_4$ in a Brønsted acidic ionic liquid. *Tetrahedron Lett*. **2007,** *48*, 8807─8810.

(47) Chu, X. Q.; Jiang, R.; Fang, Y.; Gu, Z. Y.; Meng, H.; Wang, S. Y.; Ji, S. J. Acidic-functionalized ionic liquid as an efficient, green, and metal-free catalyst for benzylation of sulfur, nitrogen, and carbon nucleophiles to benzylic alcohols. *Tetrahedron.* **2013,** *69*, 1166─1174.

(48) Kadutskii, A. P.; Kozlov, N. G.; Zhikharko, Y. D. Heterocyclization of *N*, *N*′-disubstituted p-phenylenediamines with cyclich β-diketones and formaldehyde. Synthesis of new pyrido [2, 3-g] quinoline derivatives. *Russ. J. Org. Chem.* **2011,** *47*, 412.

(49) Nişancı, B.; Ganjehyan, K.; Metin, Ö.; Daştan, A.; Türk, B. Graphene-supported NiPd alloy nanoparticles: A novel and highly efficient heterogeneous catalyst system for the reductive amination of aldehydes. *J. Mol. Catal. A: Chem.* **2015,** *409*, 191–197.

(50) Fu, M. C.; Shang, R.; Cheng, W. M.; Fu, Y. Boron-catalyzed *N*-alkylation of amines using carboxylic acids. *Angew. Chem., Int. Ed.* **2015,** *54*, 9042–9046.